"Symmetry is what we see at a glance; based on the fact that there is no reason for any difference . . ."

Blaise Pascal

3

Non-zero θ_{13} and dark matter in an S_4 flavour symmetric model with inverse seesaw

---

In this chapter we study an inverse seesaw model of neutrino mass within the framework of S_4 flavour symmetry from the requirement of generating non-zero reactor mixing angle θ_{13} along with correct dark matter relic abundance. The leading order S_4 model gives rise to tri-bimaximal type leptonic mixing resulting in $\theta_{13} = 0$. Non-zero θ_{13} is generated at one loop level by extending the model with additional scalar and fermion fields which take part in the loop correction. The particles going inside the loop are odd under an in-built $Z_2^{\rm Dark}$ symmetry such that the lightest $Z_2^{\rm Dark}$ odd particle can be a dark matter candidate. Correct neutrino and dark matter phenomenology can be achieved for such one loop corrections either to the light neutrino mass matrix or to the charged lepton mass matrix although the latter case is found to be more predictive. The predictions for neutrinoless double beta decay is also discussed and inverted hierarchy

in the charged lepton correction case is found to be disfavoured by the latest KamLAND-Zen data.

3.1 Introduction

The Standard Model (SM) of particle physics surmises on the minimal choice that a single Higgs doublet provides masses to all particles. Some questions however remain unanswered, including the origins of neutrino mass and dark matter (DM), keeping other avenues open for physics beyond the Standard Model (BSM). There have been several conclusive evidences in the last two decades which validate the existence of non-zero neutrino masses and large leptonic mixing [1–9]. The SM can not address this observed phenomena simply because the neutrinos remain massless in the model, because the SM does not accomodate any RH neutrino. If the right handed neutrinos are included by hand, one needs the Yukawa couplings to be heavily fine tuned to around 10^{-12} for the production of sub-eV neutrino masses from the same Higgs field of the SM. One can generate a tiny Majorana mass for the neutrinos from the same Higgs field of the SM at non-renormalisable level through the dimension five Weinberg operator [10]. The realisation of this dimension five operator within renormalisable theories are also available in the literature, popularly known as the seesaw mechanism [11–13]. Even if the tiny neutrino masses are produced dynamically within such seesaw frameworks, understanding the origin of the large leptonic mixing is another puzzle. Since the quark sector mixing is observed to be small, it also indicates that there may be some new dynamics operating in the leptonic sector that generates the large mixing. As we see from the global fit data, among the three mixing angles, the solar and atmospheric angles are reasonably large but the reactor angle is comparatively small. In fact, before the discovery of non-zero reactor mixing angle θ_{13} in 2012, the neutrino data were consistent with a class of neutrino mass matrices respecting $\mu - \tau$ symmetry (For a recent review, we refer [14]). This class of models predicts $\theta_{13} = 0, \theta_{23} = \frac{\pi}{4}$ whereas the value of θ_{12} depends upon the particular model. Out of different $\mu - \tau$ symmetric neutrino mass models,

the Tri-Bimaximal (TBM) mixing [15–17] received lots of attention within several neutrino mass models. The TBM mixing predicts $\theta_{12} = 35.3^o$. Such a mixing can be easily accommodated within popular discrete flavour symmetry models [18–20]. Since the measured value of θ_{13} is small, such $\mu - \tau$ symmetric models can still be considered to be valid at leading order, while the small but non-zero θ_{13} can be generated by perturbations to either the charged lepton or the neutrino sector, as studied in several works in the literature including [21–29].

On the other hand, the SM also fails to provide a particle DM candidate that can satisfy all the criteria of a good DM candidate [30]. Although there have been sufficient evidences [31–33] from astrophysics and cosmology offering the existence of DM the particle nature of DM is not yet known. This has driven the particle physics community to explore different possible BSM frameworks which can give rise to the correct DM phenomenology and can also be tested at several different experiments. Amidst them, the most popular BSM scenario is the weakly interacting massive particle (WIMP) paradigm, as the correct DM relic abundance can be achieved for such a particle if it has interaction strength similar to weak interactions. This coincidence is also referred to as the *WIMP Miracle*. The estimation on present dark matter abundance as a function of density parameter and $h = (\text{Hubble Parameter})/100$, is reported as [34]

$$\Omega_{\rm DM} h^2 = 0.1187 \pm 0.0017 \tag{3.1.1}$$

Using the measured value of Hubble parameter, this yields approximately 26% of the total energy density of the present Universe being composed of DM. The same Planck experiment also puts a bound on the sum of absolute neutrino masses $\sum_i |m_i| < 0.17$ eV [34]. Although the fundamental origin of DM may not be related to the origin of neutrino mass as well as leptonic mixing, it is pretty exciting to look for a common platform that can explain both the phenomena. In spite of keeping the BSM physics minimal, this also permits for its probe in a much larger range of experiments. We find two such frameworks very appealing: one where neutrino masses originate at one loop level with DM particles going in the loop [35] and the other where the same discrete flavour symmetry responsible for generating large leptonic mixing also guarantees a stable DM candidate [36].

More detailed phenomenology of similar models can be found in several works including [37–42]. Another recent proposal to connect dark mater with non-zero θ_{13} can be found in [43].

Motivated by this, here also we consider an inverse seesaw model [44–46] based on S_4 discrete flavour symmetry that gives rise to TBM type neutrino mixing at leading order. Unlike canonical seesaw models, the inverse seesaw can be a low scale framework where the singlet heavy neutrinos can be at or below the TeV scale without any fine tuning of Yukawa couplings. This is possible due to softly broken global lepton number symmetry by the singlet mass term as we discuss later. The existence of sterile neutrinos around TeV scale with sizeable Yukawa couplings in these models makes these models testable at planned future particle colliders [47]. Another motivation to study this particular model is the neutrino mass sum rules it predicts, which relates the three light neutrino masses [48]. This predicts the lightest neutrino mass, once the experimental data of two mass squared differences are given as input and hence can be examined at experiments perceptive to the lightest neutrino mass say, neutrinoless double beta decay (NDBD)[1]. Since the model gives rise to TBM mixing, disallowed by latest neutrino data, we extend the model in order to reproduce non-zero θ_{13} in such a way that automatically takes DM into account. For this we make use of the scotogenic mechanism [35] mentioned above where DM particles going in loop can generate tiny neutrino mass. We implement this idea in two different ways. First we add a one loop correction to the leading order light neutrino mass matrix from inverse seesaw and secondly we give a similar correction to the charged lepton mass matrix. In both the cases, the correct neutrino and DM phenomenology can be reproduced. However, the charged lepton correction is found to have advantage over the former due the fact that it does not disturb the mass sum rule prediction of the leading order model. Also, one requires less fine-tuning to generate correction to charged lepton masses due to which the lepton portal limit of inert scalar DM can be achieved, which can give different DM phenomenology compared to the well studied Higgs portal DM scenario, as

[1]For a review, please see [49]

we discuss later.

This work is organised in the following manner. In section 3.2 we summarize the S_4 based inverse seesaw model at leading order along with its predictions. In section 3.3 we explain the origin of non-zero reactor mixing angle and Dark Matter by extending the leading order model. In section 3.4 we briefly discuss DM phenomenology of the model and then briefly comment upon neutrinoless double beta decay prediction in the context of the present model in section 3.5. We discuss our results in section 3.6 and then write the conclusion in section 3.7.

3.2 Inverse Seesaw Model with S_4 Symmetry

In this section we shortly review the inverse seesaw (ISS) model and its S_4 realisation. The ISS model is an extension of the SM by two different types of singlet neutral fermions N_R, S_L three copies each. The Lagrangian reads

$$-\mathcal{L} = Y\bar{L}HN_R + M\bar{S}_L N_R + \frac{1}{2}\mu S_L S_L + \text{h.c.} \tag{3.2.1}$$

Here H represents the SM Higgs doublet and L is the lepton doublet. The presence of some additional symmetries is assumed which prevents the Majorana mass term of N_R. This Lagrangian gives rise to the following 9×9 mass matrix in the (ν_L, N_R, S_L) basis

$$M_\nu = \begin{pmatrix} 0 & m_D^T & 0 \\ m_D & 0 & M^T \\ 0 & M & \mu \end{pmatrix} \tag{3.2.2}$$

where $m_D = Y\langle h^0 \rangle$ is the Dirac neutrino mass generated by the VEV of the neutral component of the SM Higgs. Block diagonalisation of the above mass matrix results in the effective light neutrino mass matrix as ,

$$m_\nu = m_D^T (M^T)^{-1} \mu M^{-1} m_D \tag{3.2.3}$$

Unlike canonical seesaw where the light neutrino mass is inversely proportional to the lepton number violating Majorana mass term of singlet neutrinos, here the light neutrino mass is directly proportional to the singlet mass term μ. The

heavy neutrino masses are proportional to M. Here, even if $M \sim 1$ TeV, correct neutrino masses can be generated for $m_D \sim 10$ GeV, say if $\mu \sim 1$ keV. Such small μ term is natural as $\mu \to 0$ helps in recovering the global lepton number symmetry $U(1)_L$ of the model. Thus, inverse seesaw is a natural TeV scale seesaw model where the heavy neutrinos can remain as light as a TeV and Dirac mass can be as large as the charged lepton masses and can still be consistent with sub-eV light neutrino masses.

In general, the inverse seesaw formula for light neutrino mass can generate a very general structure of neutrino mass matrix. Since the leptonic mixing is found to have some specific structure with large mixing angles, one can look for possible flavour symmetry origin of it. In this context, non Abelian discrete flavour symmetries have gained lots of attention in the last few decades. For reviews and related references, please see [50, 51]. For the purpose of the present work, we are particularly interested in the inverse seesaw model proposed by [48] where the non Abelian discrete flavour symmetry is S_4 (For detail please see Section 1.8 of Chapter 1. The field content of the S_4 based inverse seesaw model is shown in Table 3.1. The additional discrete symmetry $Z_2 \times Z_3$ as well as the global $U(1)_L$ symmetry is chosen in order to generate the desired inverse seesaw mass matrix along with TBM type leptonic mixing. The lepton doublet and charged lepton singlet of the SM, the singlet neutrinos N_R, S of the inverse seesaw model transform as triplet 3_1 of S_4. The SM Higgs doublet h transform as singlet under S_4. The different flavon fields Φ's are chosen in order to get the desired mass matrices and mixing. The Yukawa Lagrangian for the particle content shown in Table 3.1 reads

$$-\mathcal{L}^I = y\bar{L}HN_R + y_M N_R S\Phi_R + y'_M N_R S\Phi'_R + y_s SS\Phi_s \qquad (3.2.4)$$

The following flavon alignments are required to get a desired neutrino mass matrix and leptonic mixing.

$$\langle\Phi_R\rangle = v_R(1,0,0),\ \langle\Phi'_R\rangle = v'_R,\ \langle\Phi_s\rangle = v_s,\ \langle H^0\rangle = v_h$$

In order to implement this flavon alignment in the inverse seesaw mechanism we note that m_D is connected to v_h and M is determined by the VEV v_R and v'_R.

	$\bar{L}$	N_R	l_R	H	S	Φ_R	Φ'_R	Φ_s	Φ_l	$\Phi_l{}'$	$\Phi_l{}''$
$SU(2)_L$	2	1	1	2	1	1	1	1	1	1	1
S_4	3_1	3_1	3_1	1_1	3_1	3_1	1_1	1_1	3_1	3_2	1_1
Z_2	+	+	+	+	-	-	-	+	+	+	+
Z_3	ω^2	ω	1	1	1	ω^2	ω^2	1	ω	ω	ω
$U(1)_L$	-1	1	1	0	-1	0	0	2	0	0	0

Table 3.1: Fields and their transformation properties under $SU(2)_L$ gauge symmetry as well as the $S_4 \times Z_2 \times Z_3 \times U(1)_L$ symmetry

In this way, the order of magnitude estimate of light neutrino mass from the Eq. (3.2.3) is $m_\nu \propto \frac{v_h^2}{(v_R+v'_R)^2}\mu$. Here v_h is of the order of electroweak symmetry breaking (EWSB) scale, v_R and v'_R can be taken of the order of TeV scale or more. Therefore, to get m_ν in sub-eV, μ which is coming from the VEV of Φ_S should be of the order of keV. Such a small vev can be naturally achieved from the soft $U(1)_L$ symmetry breaking terms in the scalar potential. For example, a term $\mu_1 \Phi_s H^\dagger H$ will generate an induced VEV of Φ_s given by $v_s = \frac{\mu_1 v_h^2}{M^2_{\Phi_s}}$. This can be adjusted to be keV by choosing a small enough μ_1. By the same naturalness argument as before, such a small μ_1 is natural. Also, since the $U(1)_L$ symmetry is explicitly broken (softly) by the scalar potential, there is no danger of generating massless Goldstone boson that can result after spontaneous breaking of global $U(1)_L$ symmetry.

Decomposition of the various terms present in the Eq. (3.2.4) into singlets can be achieved using the S_4 tensor product rules given in the Section 1.8 of Chapter 1.

$$y\bar{L}_i N_{jR} H = y(L_1 N_{1R} + L_2 N_{2R} + L_3 N_{3R}) v_h \tag{3.2.5}$$

$$\begin{aligned} y_M N_{iR} S_j \Phi_R &= y_M[(N_{2R}S_3 + N_{3R}S_2)\Phi_{1R} + (N_{1R}S_3 + N_{3R}S_1)\Phi_{2R} + (N_{1R}S_2 + N_{2R}S_1)\Phi_{3R}] \\ &= y_M[(N_{2R}S_3 + N_{3R}S_2)]v_R \end{aligned} \tag{3.2.6}$$

$$y'_M N_{iR} S_j \Phi'_R = y'_M (S_1 N_{1R} + S_2 N_{2R} + S_3 N_{3R}) v'_R \tag{3.2.7}$$

$$y_s S S \Phi_s = y_s (S_1 S_1 + S_2 S_2 + S_3 S_3) v_s \tag{3.2.8}$$

The chosen flavon alignments allow us to have different matrices involved in inverse seesaw formula as follows

$$m_D = y \begin{pmatrix} 1 & 0 & 0 \\ 0 & 1 & 0 \\ 0 & 0 & 1 \end{pmatrix} v_h,\ \mu = y_s \begin{pmatrix} 1 & 0 & 0 \\ 0 & 1 & 0 \\ 0 & 0 & 1 \end{pmatrix} v_s,\ M = \begin{pmatrix} y'_M v'_R & 0 & 0 \\ 0 & y'_M v'_R & y_M v_R \\ 0 & y_M v_R & y'_M v'_R \end{pmatrix} \tag{3.2.9}$$

The above three matrices lead to the following light neutrino mass matrix under ISS framework

$$m_\nu = U_\nu m_\nu^{o(diag)} U_\nu^T. \tag{3.2.10}$$

Using Eq. (3.2.9) in Eq. (3.2.3) the light neutrino mass matrix is found to be

$$m_\nu^o = \begin{pmatrix} \frac{1}{a^2} & 0 & 0 \\ 0 & \frac{a^2+b^2}{(b^2-a^2)^2} & -\frac{2ab}{(b^2-a^2)^2} \\ 0 & -\frac{2ab}{(b^2-a^2)^2} & \frac{a^2+b^2}{(b^2-a^2)^2} \end{pmatrix} \tag{3.2.11}$$

where, $a = y'_M v'_R/(\sqrt{y_s v_s} y v_h)$ and $b = y_M v_R/(\sqrt{y_s v_s} y v_h)$. The eigenvalues of this light neutrino mass matrix are

$$m_1 = \frac{1}{(a+b)^2},\ m_2 = \frac{1}{(a-b)^2},\ m_3 = \frac{1}{a^2}$$

which satisfy the neutrino mass sum rule

$$\frac{1}{\sqrt{m_1}} = \frac{2}{\sqrt{m_3}} - \frac{1}{\sqrt{m_2}} \tag{3.2.12}$$

Now the Lagrangian for the charged leptons can be written in terms of dimension five operators as [48]

$$-\mathcal{L}^l = \frac{y_l}{\Lambda} \bar{L} l_R H \Phi_l + \frac{y_l{}'}{\Lambda} \bar{L} l_R H \Phi_l{}' + \frac{y_l{}''}{\Lambda} \bar{L} l_R H \Phi_l{}'' \tag{3.2.13}$$

The authors of [48] considered additional messenger fields χ, χ^c such that this effective Lagrangian for charged leptons can be obtained after integrating out these heavy messenger fields. The following flavon alignments allow us to have the desired mass matrix corresponding to the charged lepton sector

$$\langle \Phi_l \rangle = v_l(1,1,1),\ \langle \Phi_l{}' \rangle = v_l{}'(1,1,1),\ \langle \Phi_l{}'' \rangle = v_l{}''$$

The charged lepton mass matrix is then given by

$$m_l^0 = \begin{pmatrix} y_l'' v_l'' & y_l v_l - y_l' v_l' & y_l v_l + y_l' v_l' \\ y_l v_l + y_l' v_l' & y_l'' v_l'' & y_l v_l - y_l' v_l' \\ y_l v_l - y_l' v_l' & y_l v_l + y_l' v_l' & y_l'' v_l'' \end{pmatrix} \frac{v_h}{\Lambda} \tag{3.2.14}$$

As mentioned in [52] the charge lepton mass matrix m_l is diagonalised on the left by the magic matrix U_ω given by

$$U_\omega = 1/\sqrt{3} \begin{pmatrix} 1 & 1 & 1 \\ 1 & \omega & \omega^2 \\ 1 & \omega^2 & \omega \end{pmatrix}, \tag{3.2.15}$$

(with $\omega = \exp 2i\pi/3$). Now we know that the leptonic mixing matrix is given by

$$U = U_{\rm TBM} = U_l^\dagger U_\nu$$

where U_l corresponds to the identity matrix if the charged lepton mass matrix is diagonal. Since in our work, the charged lepton mass matrix is non-diagonal and is nothing but the magic matrix U_ω given by Eq. (3.2.15), the leptonic mixing matrix is

$$U_{\rm TBM} = U_\omega^\dagger U_\nu$$

The desired structures of the mass and mixing matrices written above have been made possible due to chosen flavour symmetries of the theory. For example, as required by the structure of the inverse seesaw mass matrix given in Eq. (3.2.2), there should not be any mass term involving ν_L and S. However, the coupling between ν_L and S is not forbidden by the SM gauge symmetry as well as S_4 flavour symmetry. In this regard, the additional $Z_2 \times Z_3$ symmetry and the chosen charges of ν_L, S under it keep the unwanted coupling of ν_L and S through the Higgs doublet H away. Similarly, the (22) term of the inverse seesaw mass matrix (3.2.2) or the mass term involving N_R, N_R should also be forbidden. However, the SM gauge symmetry as well as the S_4 flavour symmetry and $U(1)_L$ global symmetry can not prevent a term like $\Phi_s N_R N_R$ which will introduce a non-zero (22) entry into the inverse seesaw mass matrix. Therefore, the additional $Z_2 \times Z_3$ symmetry and non-trivial charges of N_R under this has to be chosen to keep such

a term away from the Lagrangian. As mentioned above, the approximate $U(1)_L$ global symmetry helps in generating small (33) entry of the inverse seesaw mass matrix naturally, without any fine tuning of parameters. Thus, all the additional symmetries $Z_2 \times Z_3 \times U(1)_L$ play a crucial role in generating the desired structure of the inverse seesaw mass matrix along with the desired leptonic mixing.

3.3 Origin of non-zero θ_{13} and dark matter

Since $\theta_{13} = 0$ has already been ruled out by several neutrino experiments, one has to go beyond the TBM framework discussed in the previous work. This can simply be done in two different ways: giving corrections to the neutrino mass matrix or the charged lepton mass matrix. Both of these corrections will change the leptonic mixing matrix in a way to generate non-zero θ_{13}.

3.3.1 Correction to neutrino mass matrix

The model discussed above can be extended by the particle content shown in Table 3.2 charged under an additional Z_2^{Dark} symmetry guaranteeing the stability of the dark matter candidate. This additional field content will introduce a few

	$SU(2)_L$	S_4	Z_2	Z_3	$U(1)_L$	Z_2^{Dark}
η	2	1	1	1	0	-1
ψ_R	1	3	1	ω	1	-1
Φ'_s	1	1	1	ω	-2	1
Φ_ψ	1	3	1	ω	-2	1

Table 3.2: Fields responsible for generating non-zero θ_{13} as well as dark matter with their respective transformations under the symmetry group of the model.

more terms in the Yukawa Lagrangian given as

$$\mathcal{L}^I \supset h\bar{L}\psi_R\eta + y_\psi\psi_R\psi_R\Phi'_s + y'\psi_R\psi_R\Phi_\psi \tag{3.3.1}$$

The extra scalar doublet η odd under the Z_2^{Dark} symmetry introduces several other terms in the scalar potential. The most relevant terms are the interactions

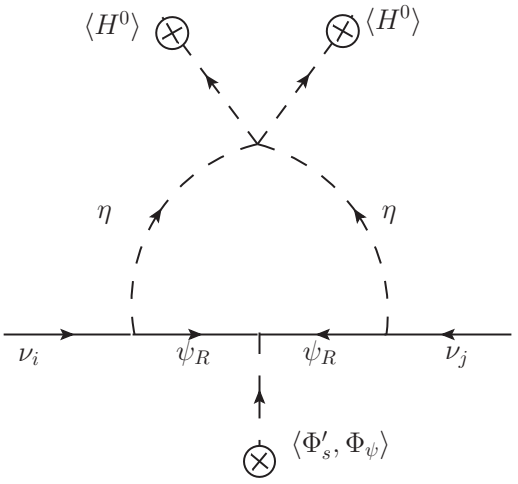

Figure 3.1: Radiative generation of non-zero θ_{13} from the light neutrino sector

with the standard model Higgs h which are relevant for neutrino mass and dark matter analysis. These relevant terms of the scalar potential can be written as

$$V(H,\eta) \supset \mu_1^2|H|^2 + \mu_2^2|\eta|^2 + \frac{\lambda_1}{2}|H|^4 + \frac{\lambda_2}{2}|\eta|^4 + \lambda_3|H|^2|\eta|^2 + \lambda_4|H^\dagger\eta|^2 + \{\frac{\lambda_5}{2}(H^\dagger\eta)^2 + \text{h.c.}\} \tag{3.3.2}$$

Using the expression from [35] of one-loop neutrino mass

$$(m_\nu)_{ij} = \frac{h_{ik}h_{jk}M_k}{16\pi^2}\left(\frac{m_R^2}{m_R^2 - M_k^2}\ln\frac{m_R^2}{M_k^2} - \frac{m_I^2}{m_I^2 - M_k^2}\ln\frac{m_I^2}{M_k^2}\right) \tag{3.3.3}$$

Here $m_{R,I}^2$ are the masses of scalar and pseudoscalar part of η^0 and M_k the mass of singlet fermion ψ_R in the internal line. The index $i,j = 1,2,3$ runs over the three fermion generations as well as three copies of ψ. For $m_R^2 + m_I^2 \approx M_k^2$, the above expression can be simply written as

$$(m_\nu)_{ij} \approx \frac{\lambda_5 v_h^2}{32\pi^2}\frac{h_{ik}h_{jk}}{M_k} = \frac{m_I^2 - m_R^2}{32\pi^2}\frac{h_{ik}h_{jk}}{M_k} \tag{3.3.4}$$

where $m_I^2 - m_R^2 = \lambda_5 v_h^2$ is assumed ignoring the quartic terms of η with other flavon fields. This formula for light neutrino mass is written in a basis where the mass matrix of the intermediate fermion ψ is diagonal which is true if only Φ'_s contributes to its mass $M_k = y_\psi\langle\Phi'_s\rangle$ due to the structure of S_4 tensor product $\psi_R\psi_R\Phi'_s = (\psi_{R1}\psi_{R1} + \psi_{R2}\psi_{R2} + \psi_{R3}\psi_{R3})\Phi'_s$. However, due to the S_4 triplet assignment to the other scalar Φ_ψ, the mass matrix of ψ_R becomes non-diagonal

of the form

$$M_\psi = \begin{pmatrix} y_\psi v'_s & y'_\psi v_{\psi 3} & y'_\psi v_{\psi 2} \\ y'_\psi v_{\psi 3} & y_\psi v'_s & y'_\psi v_{\psi 1} \\ y'_\psi v_{\psi 2} & y'_\psi v_{\psi 1} & y_\psi v'_s \end{pmatrix}, \tag{3.3.5}$$

where $\langle \Phi_\psi \rangle = (v_{\psi 1}, v_{\psi 2}, v_{\psi 3})$ is the vacuum alignment of the flavon field Φ_ψ. Also the S_4 product rules dictate the Yukawa matrix h_{ij} to be diagonal in flavour space. Therefore, the new contribution to the light neutrino mass matrix will assume a structure similar to M_ψ. We can parameterise this correction, in general as

$$\delta m_\nu = \begin{pmatrix} x_\nu & y_\nu & z_\nu \\ y_\nu & x_\nu & w_\nu \\ z_\nu & w_\nu & x_\nu \end{pmatrix} \tag{3.3.6}$$

In this particular setup, the fermion ψ_R carries lepton number, and since lepton number is only softly broken within an inverse seesaw framework, one expects the VEV's of Φ'_s, Φ_ψ to be small say, of the order of keV in a TeV scale inverse seesaw model discussed above. Therefore, the dark matter in this model is a keV singlet fermion ψ_R. On the other hand, if ψ_R does not carry a lepton number, then the scalar doublet η carries a lepton number and the one-loop contribution can be generated with the particle content shown in Table 3.3. The Yukawa

	$SU(2)_L$	S_4	Z_2	Z_3	$U(1)_L$	Z_2^{Dark}
η	2	1	1	1	1	-1
ψ_R	1	3	1	ω	0	-1
Φ'_s	1	1	1	ω	0	1
Φ_ψ	1	3	1	ω	0	1
Δ_L	3	1	1	1	0	1

Table 3.3: Fields responsible for generating non-zero θ_{13} as well as dark matter with their respective transformations under the symmetry group of the model.

Lagrangian corresponding to this new field content is

$$\mathcal{L}^I \supset h\bar{L}\psi_R\eta + y_\psi \psi_R \psi_R \Phi'_s + y'\psi_R\psi_R\Phi_\psi \tag{3.3.7}$$

These relevant terms of the scalar potential can be written as

$$V(H,\eta,\Delta_L) \supset \mu_1^2|H|^2 + \mu_2^2|\eta|^2 + \frac{\lambda_1}{2}|H|^4 + \frac{\lambda_2}{2}|\eta|^4 + \lambda_3|H|^2|\eta|^2 + \lambda_4|H^\dagger\eta|^2 \tag{3.3.8}$$

$$+ \{\frac{\lambda_5}{2}\eta^2\Delta_L\Phi_s + \text{h.c.}\}, \tag{3.3.9}$$

In this case, the fermion ψ_R can acquire a diagonal mass term due to the coupling with Φ_s' flavon and also acquire non diagonal mass terms from the flavon field Φ_ψ. The combined mass matrix for ψ_R therefore, has a similar structure to the one shown in Eq. (3.3.5). Since neither ψ_R nor Φ_ψ carries any lepton number, their mass and VEV respectively are not constrained to be small from naturalness argument. Also, the triplet scalar Δ_L does not couple to the leptons at tree level as it does not carry any lepton number. The corresponding neutrino mass diagram at one loop is shown in figure 3.2. This is equivalent to a radiative type II seesaw mechanism. In this case, the scalar doublet η can be naturally lighter than ψ_R and hence can be a dark matter candidate. We discuss this dark matter candidate in details later, specially with reference to its interactions with the light neutrinos, responsible for generating non-zero θ_{13}. In both these cases, the correction to the light neutrino mass matrix can be parameterised as Eq. (3.3.6). One can then write down the complete light neutrino mass matrix as

$$m_\nu = m_\nu^0 + \delta m_\nu = U_{\text{PMNS}} m_\nu^{\text{diag}} U_{\text{PMNS}}^T \tag{3.3.10}$$

where the Pontecorvo-Maki-Nakagawa-Sakata (PMNS) leptonic mixing matrix can be parametrized as

$$U_{\text{PMNS}} = \begin{pmatrix} c_{12}c_{13} & s_{12}c_{13} & s_{13}e^{-i\delta} \\ -s_{12}c_{23} - c_{12}s_{23}s_{13}e^{i\delta} & c_{12}c_{23} - s_{12}s_{23}s_{13}e^{i\delta} & s_{23}c_{13} \\ s_{12}s_{23} - c_{12}c_{23}s_{13}e^{i\delta} & -c_{12}s_{23} - s_{12}c_{23}s_{13}e^{i\delta} & c_{23}c_{13} \end{pmatrix} U_{\text{Maj}} \tag{3.3.11}$$

where $c_{ij} = \cos\theta_{ij}$, $s_{ij} = \sin\theta_{ij}$ and δ is the leptonic Dirac CP phase. The diagonal matrix $U_{\text{Maj}} = \text{diag}(1, e^{i\alpha}, e^{i(\beta+\delta)})$ contains the Majorana CP phases α, β which remained unknown. For NH, we can write $m_\nu^{\text{diag}} = \text{diag}(m_1, \sqrt{m_1^2 + \Delta m_{21}^2}, \sqrt{m_1^2 + \Delta m_{31}^2})$ and $m_\nu^{\text{diag}} = \text{diag}(\sqrt{m_3^2 + \Delta m_{23}^2 - \Delta m_{21}^2}, \sqrt{m_3^2 + \Delta m_{23}^2}, m_3)$ for

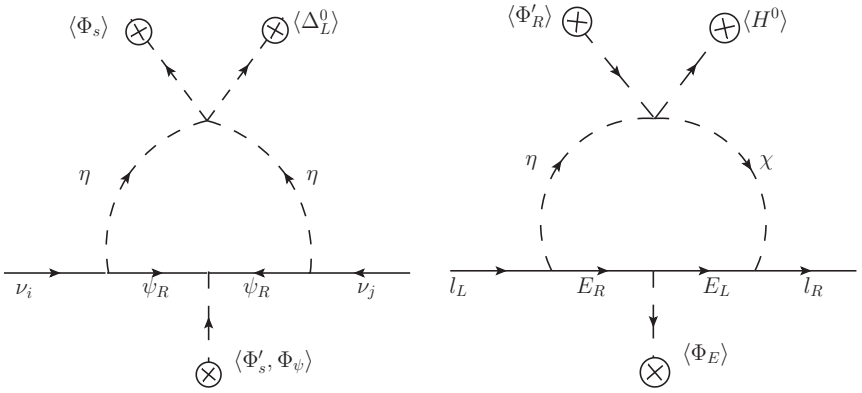

Figure 3.2: Radiative generation of non-zero θ_{13} from the light neutrino sector (left panel) and charged lepton sector (right panel)

IH. Using the 3σ values of neutrino parameters, we can find the model parameters in $m_\nu^0 + \delta m_\nu$ which can give rise to the correct neutrino phenomenology.

3.3.2 Correction to charged lepton mass matrix

Similar to the above, one can also give a radiative correction to the charged lepton mass matrix, by considering the presence of vector like charged fermions instead of neutral ones. The relevant particle content is shown in Table 3.4. The Yukawa Lagrangian corresponding to this new field content is

$$\mathcal{L}^I \supset h\bar{L}E_R\eta^\dagger + h'\bar{l}_R E_L\chi + M_E\bar{E}_L E_R + y_E\Phi_E\bar{E}_L E_R \tag{3.3.12}$$

These relevant terms of the scalar potential can be written as

$$\begin{aligned} V \supset\ & \mu_1^2|H|^2 + \mu_2^2|\eta|^2 + \frac{\lambda_1}{2}|H|^4 + \frac{\lambda_2}{2}|\eta|^4 + \lambda_3|H|^2|\eta|^2 + \lambda_4|H^\dagger\eta|^2 \\ & + \{\frac{\lambda_5}{2}(H^\dagger\eta)^2 + \text{h.c.}\} + \lambda_6 H^\dagger\eta\chi^\dagger\Phi'_R \end{aligned} \tag{3.3.13}$$

The corresponding Feynman diagram for one-loop charged lepton mass is shown in figure 3.2 (right panel). One can write down the one-loop expression similar to the one written for one-loop neutrino masses. Here also, the mass matrix of vector like charged leptons acquire a similar structure as shown for neutral fermion ψ_R in Eq. (3.3.5). Also the Yukawa matrix related to the coupling of $\bar{l}_L E_R\eta$ or $\bar{l}_R E_L\chi$ is restricted to be diagonal due to S_4 product rules. Therefore,

one can parameterise the correction to the charged lepton mass matrix as

$$\delta m_l = \begin{pmatrix} a_l & b_l & c_l \\ b_l^s & a_l & d_l \\ c_l^s & d_l^s & a_l \end{pmatrix} \tag{3.3.14}$$

Adding this correction to the leading order charged lepton mass matrix given

	$SU(2)_L$	S_4	Z_2	Z_3	$U(1)_L$	$Z_2^{\rm Dark}$
η	2	1	1	1	0	-1
χ	1	1	1	ω^2	0	-1
$E_{L,R}$	1	3	1	ω	1	-1
Φ_E	1	3	1	1	0	1

Table 3.4: Fields responsible for generating non-zero θ_{13} as well as dark matter with their respective transformations under the symmetry group of the model.

in Eq. (3.2.14) should give rise to a different diagonalising matrix U_l of charged leptons. The structure of this matrix will depend upon the parameters a_l, b_l, c_l, d_l which can be constrained from the requirement of producing the correct leptonic mixing matrix after multiplying with U_ν, the diagonalising matrix of light neutrino mass matrix. From the tree level model one can find $U_\nu = U_\omega U_{\rm TBM}$. Now, the total charged lepton mass matrix is

$$m_l = m_l^0 + \delta m_l = U_L m_l^{\rm diag} U_R^\dagger \tag{3.3.15}$$

where $U_{L,R}$ are unitary matrices that can diagonalise the complex charged lepton mass matrix. Here $m_l^{\rm diag}$ is the known diagonal charged lepton mass matrix. The unitary matrix U_L goes into the observed leptonic mixing matrix and hence can be calculated as $U_L = U_\nu U_{\rm PMNS}^\dagger$ which can be written in terms of known U_ν from the leading order model and the known PMNS mixing matrix. We parameterise the another unitary matrix U_R in terms of three mixing angles and one phase and vary them randomly in $0 - \pi/4$ for angles and $0 - 2\pi$ for phase. Thus, we can calculate the charged lepton mass matrix in terms of known parameters as well as randomly generated values of U_R. For each possible such charged lepton mass matrix, we can then solve the above Eq. (3.3.15) and calculate the model

parameters such that correct leptonic mixing can be achieved. In this model, the dark matter candidate can either be a scalar doublet η or a scalar singlet χ. We discuss their dark matter phenomenology below specially with reference to their interactions with the charged leptons.

3.4 Dark matter

In the very early epochs of the Universe, the abundance of a typical WIMP DM relic particle (η) is usually taken to be the equilibrium abundance. When the temperature of the radiation dominated Universe cools down below $T \sim m_\eta$, η becomes non-relativistic and quickly after that it also decouples from the thermal bath and its abundance freezes out. The final relic abundance of such a particle η which was in thermal equilibrium at earlier epochs can be calculated by solving the Boltzmann equation

$$\frac{dn_\eta}{dt} + 3Hn_\eta = -\langle\sigma v\rangle(n_\eta^2 - (n_\eta^{\rm eqb})^2) \tag{3.4.1}$$

where n_η is the number density of the DM particle η and $n_\eta^{\rm eqb}$ is the equilibrium number density. Also, H is the Hubble expansion rate of the Universe and $\langle\sigma v\rangle$ is the thermally averaged annihilation cross-section of the DM particle η. It is clear from this equation that when η was in thermal equilibrium, the right hand side of it vanishes and the number density of DM decreases with time only due to the expansion of the Universe, as expected. The approximate analytical solution of the above Boltzmann equation gives [53, 54]

$$\Omega_\chi h^2 \approx \frac{1.04 \times 10^9 x_F}{M_{Pl}\sqrt{g_*}(a + 3b/x_F)} \tag{3.4.2}$$

where $x_F = m_\chi/T_F$, T_F is the freeze-out temperature, g_* is the number of relativistic degrees of freedom at the time of freeze-out and $M_{Pl} \approx 10^{19}$ GeV is the Planck mass. Here, x_F can be calculated from the iterative relation

$$x_F = \ln \frac{0.038 g M_{\rm Pl} m_\chi < \sigma v >}{g_*^{1/2} x_F^{1/2}} \tag{3.4.3}$$

Typically, DM particles with electroweak scale mass and couplings freeze out at temperatures in the range $x_F \approx 20 - 30$. The expression for relic density also

has a more simplified form given as [55]

$$\Omega_\chi h^2 \approx \frac{3 \times 10^{-27} \mathrm{cm}^3 \mathrm{s}^{-1}}{\langle \sigma v \rangle} \tag{3.4.4}$$

In the model discussed in the previous section, there can be two different types of DM candidates, the lightest neutral particle under the Z_2^{Dark} symmetry. In the model with corrections to neutrino sector, either the neutral fermion ψ_R or the neutral component of the scalar doublet η can be DM depending on their masses whereas in the latter model with corrections to the charged lepton sector, only the scalar DM is possible. To keep the discussion same for both these models, we briefly discuss scalar DM phenomenology in this work. The scalar DM relic abundance calculation has already been done in several works [56–60]. Typically, correct relic abundance can be satisfied for two regions of DM mass in such a model: one below the W boson mass threshold and another around 550 GeV or more. Here we focus mainly on the low mass regime where the dominant annihilation channel of DM is the one through Higgs portal interactions. Also, depending on the mass difference between different components of the scalar doublet η, coannihilations can also play a non-trivial role. In the limit where Higgs portal and coannihilation effects are sub-dominant, the DM can annihilate through the lepton portal interactions which are also relevant for correct neutrino phenomenology discussed above. Here we briefly comment on the lepton portal interaction and its role in generating DM relic abundance using the approximate analytical formula mentioned above.

It is straightforward to see from the Lagrangian that the scalar DM can annihilate into leptons through a process mediated by heavy fermions ψ or $E_{L,R}$. The corresponding annihilation cross-section is given by [61]

$$\sigma v = \frac{v^2 h^4 m_\eta^2}{48\pi (m_\eta^2 + m_\psi^2)^2} \tag{3.4.5}$$

With $v \sim 0.3c$ is the typical relative velocity of the two DM particles at the freeze out temperature, η is the relic particle (DM), h is the Yukawa coupling, m_η the relic mass, m_ψ is the mass of the gauge singlet mediating the annihilation. We then vary the DM mass and the Yukawa coupling for different benchmark values of mediator masses and constrain the parameter space from the requirement

of generating the correct DM relic abundance. It should be noted that, there are also constraints from DM direct detection experiments like LUX [62] which currently rules out DM-nucleon spin independent cross section above around 2.2×10^{-46} cm^2 for DM mass of around 50 GeV. However, the lepton portal interactions can not mediate DM-nucleon interactions and hence such bounds are weak in these cases. In fact, such null results at direct detection experiments will push lepton portal interactions of DM into a more favourable regime.

3.5 Neutrinoless double beta decay

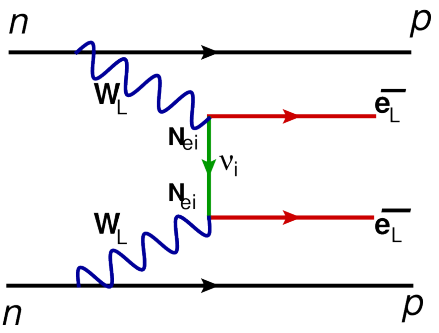

Figure 3.3: Feynman diagram contributing to neutrinoless double beta decay due to light Majorana neutrino exchanges [14].

The neutrinoless double beta decay (NDBD) is a lepton number violating process where a heavier nucleus decays into a lighter one and two electrons $(A, Z) \rightarrow (A, Z+2)+2e^-$ without any antineutrinos in the final state. If the light neutrinos of SM are Majorana fermions, then they can contribute to NDBD through the interactions shown in the Feynman diagram of figure 3.3. The amplitude of this light neutrino contribution is

$$A_{\nu LL} \propto G_F^2 \sum_i \frac{m_i U_{ei}^2}{p^2} \tag{3.5.1}$$

with p being the average momentum exchange for the process. In the above expression, m_i are the masses of light neutrinos for $i = 1, 2, 3$ and U is the PMNS leptonic mixing matrix mentioned earlier. The corresponding half-life of

neutrinoless double beta decay can be written as

$$\frac{1}{T^{0\nu}_{1/2}} = G^{0\nu}_{01}\left(|\mathcal{M}^{0\nu}_{\nu}(\eta^{L}_{\nu})|^2\right) \tag{3.5.2}$$

where $\eta^{L}_{\nu} = \sum_i \frac{m_i U^2_{ei}}{m_e}$ with m_e being the mass of electron. Also, $\mathcal{M}^{0\nu}_{\nu}$ is the nuclear matrix element. The recent bound from the KamLAND-Zen experiment constrains $0\nu\beta\beta$ half-life [63]

$$T^{0\nu}_{1/2}(\text{Xe136}) > 1.1 \times 10^{26}\ \text{yr}$$

which is equivalent to $|M^{ee}_{\nu}| < (0.06 - 0.16)$ eV at 90% C.L. where M^{ee}_{ν} is the effective neutrino mass given by

$$M^{ee}_{\nu} = U^2_{ei} m_i \tag{3.5.3}$$

Here U_{ei} are the elements of the first row of the PMNS mixing matrix. More explicitly, it is given by

$$M^{ee}_{\nu} = m_1 c^2_{12} c^2_{13} + m_2 s^2_{12} c^2_{13} e^{2i\alpha} + m_3 s^2_{13} e^{2i\beta} \tag{3.5.4}$$

Thus, the NDBD half-life is sensitive to the Majorana phases and the lightest neutrino mass as well, which remain undetermined at neutrino oscillation experiments. In the present model, the light neutrino contribution is the only dominant contribution. We check the predictions of our model for NDBD effective mass for both the cases and compare with the experimental bounds.

Parameters	Normal Hierarchy (NH)	Inverted Hierarchy (IH)
$\frac{\Delta m^2_{21}}{10^{-5}\text{eV}^2}$	$7.03 - 8.09$	$7.02 - 8.09$
$\frac{\lvert\Delta m^2_{3l}\rvert}{10^{-3}\text{eV}^2}$	$2.407 - 2.643$	$2.399 - 2.635$
$\sin^2\theta_{12}$	$0.271 - 0.345$	$0.271 - 0.345$
$\sin^2\theta_{23}$	$0.385 - 0.635$	$0.393 - 0.640$
$\sin^2\theta_{13}$	$0.01934 - 0.02392$	$0.01953 - 0.02408$
δ	$0^\circ - 360^\circ$	$145^\circ - 390^\circ$

Table 3.5: Global fit 3σ values of neutrino oscillation parameters [64]. Here $\Delta m^2_{3l} \equiv \Delta m^2_{31}$ for NH and $\Delta m^2_{3l} \equiv \Delta m^2_{32}$ for IH.

3.6 Results and discussions

We first parametrize the light neutrino mass matrix in terms of the 3σ global fit data available [64] which are summarised in Table 3.5. For the correction to the neutrino sector case, we then use Eq. (3.3.10) to relate the light neutrino mass matrix predicted by the model with the one parametrized by the global fit data. The leading order neutrino mass matrix given by Eq. (3.2.11) contains two complex parameters a, b whereas the correction to light neutrino mass is made up of four complex parameters x, y, z, w as seen from Eq. (3.3.6). The parametric form of light neutrino mass matrix is complex symmetric and hence contains six complex elements. Therefore, one can exactly solve the system of equations arising from Eq. (3.3.10) in order to evaluate the model parameters in terms of the known neutrino parameters. To be more precise, there are in fact five complex equations and one constraints arising from Eq. (3.3.10). This is due to the fact that in the total neutrino mass matrix predicted by the model, we have the 22 and 33 entries equal. This in fact restricts the light neutrino parameters, as it gives rise to two real equations involving the light neutrino parameters. We first solve these system of equations and generate the light neutrino parameters which satisfy them. For the resulting light neutrino parameters, we solve the other five complex equations to evaluate the model parameters. Since we have six model parameters and only five equations now, we vary the parameter x in the correction term (3.3.6) randomly in a range $10^{-6} - 10^{-1}$ eV. Since there are nine neutrino parameters namely, three masses, three angles and three phases, one can in general, show the variation of model parameters in terms of all of these nine parameters which are being varied randomly in their allowed ranges. Here we show only a few of them for illustrative purposes. For example, we show the variation of some of the model parameters in terms of the light neutrino parameters in figure 3.4, 3.5, 3.6, 3.7 and 3.8. This shows that the model parameters in the leading order and the correction mass matrices can not be arbitrary, but have to be within some specific ranges in order to be consistent with correct light neutrino data. From the figures 3.4 and 3.5 it is seen that the parameters of the leading order light neutrino mass matrix are in the range

$a, b \approx 1 - 10$ eV$^{-1/2}$. We recall the expressions for a, b in terms of the model parameters $a = y'_M v'_R/(\sqrt{y_s v_s} y v_h)$ and $b = y_M v_R/(\sqrt{y_s v_s} y v_h)$ mentioned earlier. Taking the lepton number violating term $\mu = y_s v_s \approx 1$ keV, the VEV of Higgs doublet at electroweak scale $v_h \approx 100$ GeV and the VEV of the other scalars Φ_R, Φ'_R around a TeV that is, $v_R, v'_R \approx 1$ TeV, our numerical results suggest that

$$\frac{y_M}{y} = \frac{y'_M}{y} \approx 10 - 1000 \tag{3.6.1}$$

in order to satisfy the correct neutrino data. This can be achieved by suitable tuning of the Dirac Yukawa y relative to $y_M = y'_M$. On the other hand, from the figures 3.6, 3.7 and 3.8, it can be seen that the correction terms to the light neutrino mass matrix lie in the sub-eV regime. The one loop correction term shown in Eq. (3.3.3) can be approximated for $m_R^2 + m_I^2 \approx M_k^2$, the above expression can be simply written as

$$(m_\nu)_{ij} \approx \frac{\lambda_5 v_h^2}{32\pi^2} \frac{h_{ik} h_{jk}}{M_k} = \frac{m_I^2 - m_R^2}{32\pi^2} \frac{h_{ik} h_{jk}}{M_k} \tag{3.6.2}$$

If the heavy neutrino mass M_k is around a TeV, then for $m_I^2 - m_R^2 \approx 1$ GeV, one can generate sub eV scale corrections ~ 0.01 eV if the corresponding Yukawa couplings are fine tuned to $h \approx 10^{-3}$. In the model with corrections to the leading order charged lepton mass matrix, we first find out the diagonalising matrix of light neutrino mass matrix as $U_\nu = U_\omega U_{\rm TBM}$ using the leading order results mentioned before. Since the light neutrino mass matrix remains the same after the charged lepton correction, U_ν also remains same. However the addition of correction will change the left diagonalising matrix of charged lepton mass matrix from the magic matrix U_ω to something else, denoted by $U_L = U_\nu U_{\rm PMNS}^\dagger$. Now, using Eq. (3.3.15), one can relate the complete charged lepton mass matrix predicted by the model, with the parametrized one given by the right hand side of Eq. (3.3.15). The total charged lepton mass matrix can be written as

$$m_l = m_l^0 + \delta m_l = \begin{pmatrix} x + a_l & y - z + b_l & y + z + c_l \\ y + z + b_l^s & x + a_l & y - z + d_l \\ y - z + c_l^s & y + z + d_l^s & x + a_l \end{pmatrix} \tag{3.6.3}$$

which contains ten complex parameters. Here x, y, z correspond to $y_l'' v_l'', y_l v_l, y_l' v_l'$ respectively in the leading order charged lepton mass matrix (3.2.14). Also there

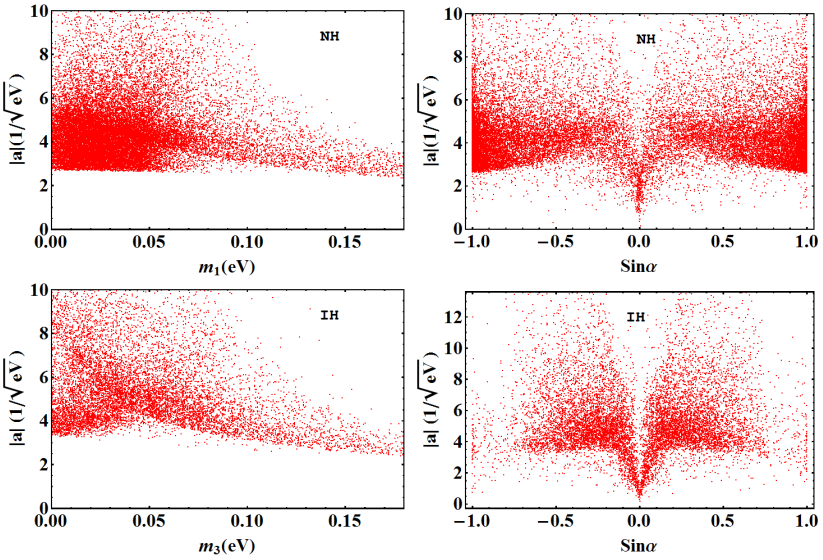

Figure 3.4: Model parameter as a function of the lightest neutrino mass and Majorana phase α.

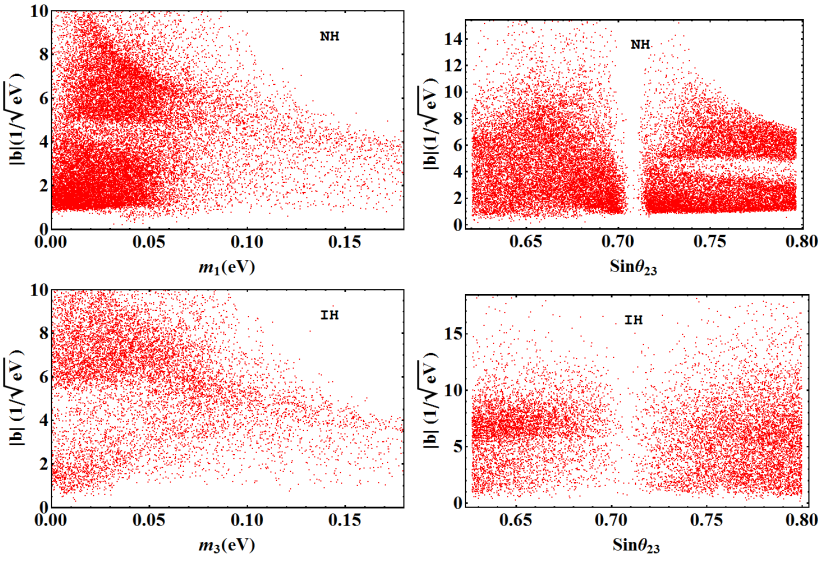

Figure 3.5: Model parameters as a function of the lightest neutrino mass and the atmospheric mixing angle θ_{23}.

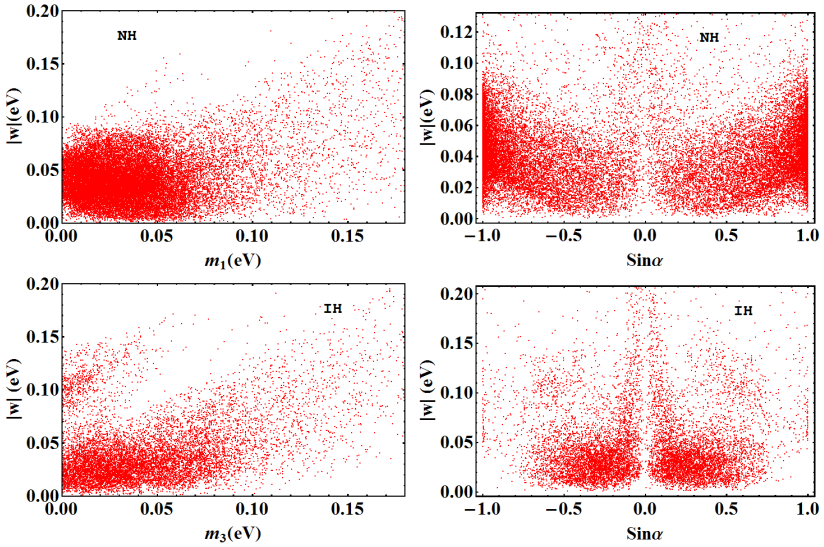

Figure 3.6: Corrections parameter(correction to neutrino mass matrix) as a function of lightest neutrino mass and Majorana phase α.

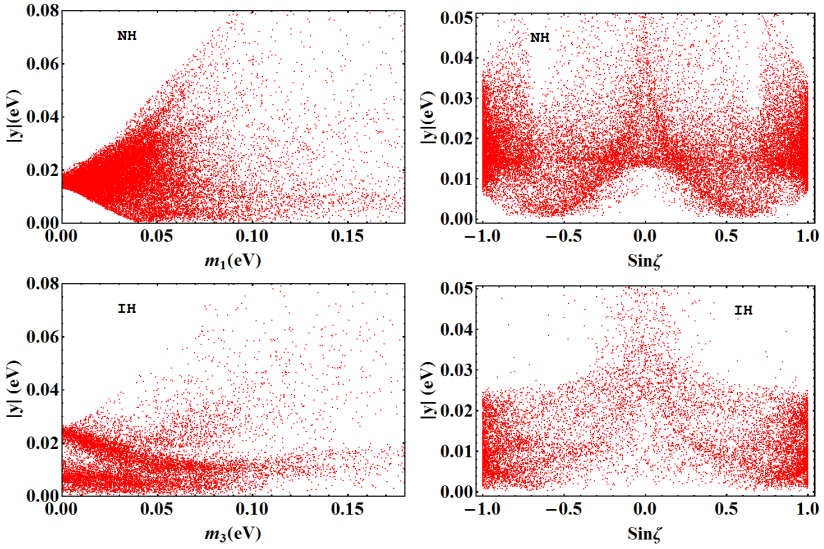

Figure 3.7: Corrections parameter(correction to neutrino mass matrix) as a function of lightest neutrino mass and Majorana phase ζ.

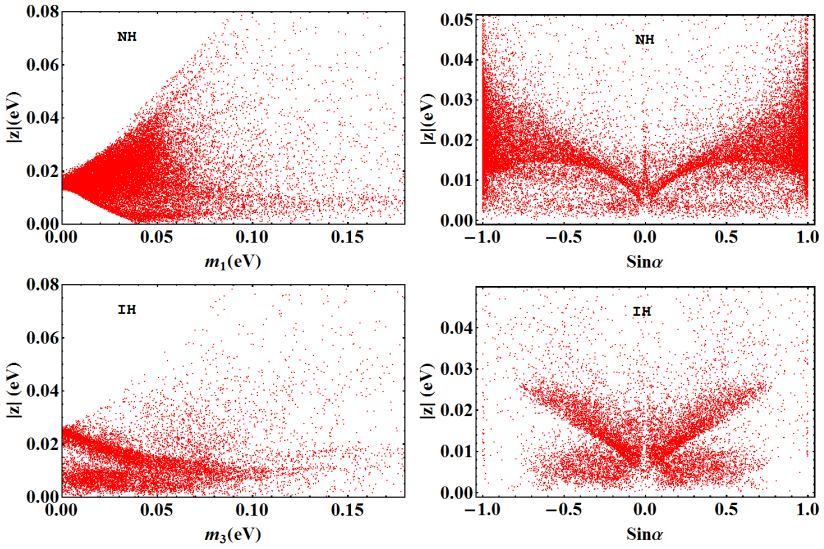

Figure 3.8: Corrections parameter(correction to neutrino mass matrix) as a function of lightest neutrino mass and Majorana phase α.

are two constraints in the parametrized charged lepton mass matrix due to fact that the 11, 22 and 33 elements are equal. This severely constraints the mixing angles and phases. Since the angles contained in U_L are related to the PMNS mixing angles, they can not be tuned arbitrarily. This forces some of the angles in U_R to take very small values in order to satisfy these two constraints. The tiny values are required in order to compensate for the large hierarchy in charged lepton masses which enters the 11, 22 and 33 elements of the mass matrix. We first solve these constraints numerically and then find the model parameters for those allowed values of mixing angles. We vary x, y, z randomly in $10^{-6} - 1.0$ GeV and evaluate other model parameters $a_l, b_l, c_l, d_l, b_l^s, c_l^s, d_l^s$ from the requirement of producing the correct leptonic mixing data. Unlike the earlier model with corrections to the neutrino mass matrix, here we get very few number of allowed points. For illustrative purposes we show the variation of a_l, b_l, c_l, d_l with some light neutrino parameters in figure 3.9 and 3.10. Since these one loop correction terms lie in the sub GeV regime, one can generate them without much fine tuning in the corresponding Yukawa couplings. For the same set of allowed parame-

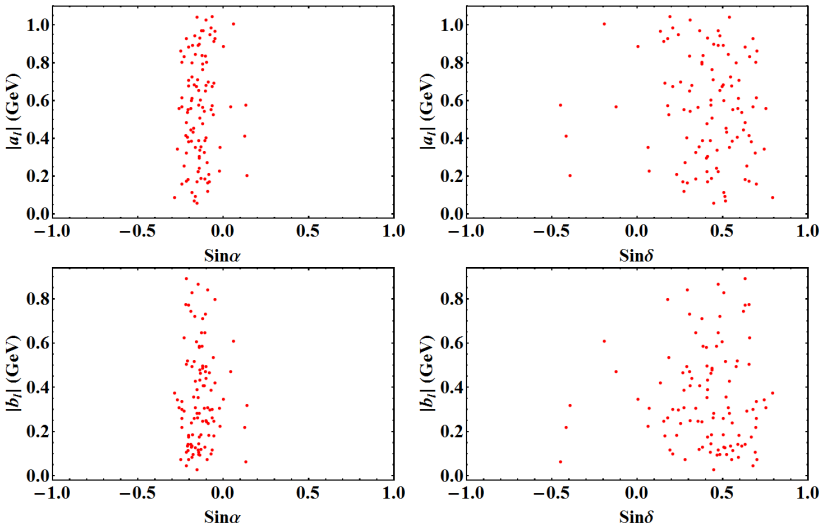

Figure 3.9: Correction parameters as a function of Majorana and Dirac phases while giving correction to the charged lepton mass matrix.

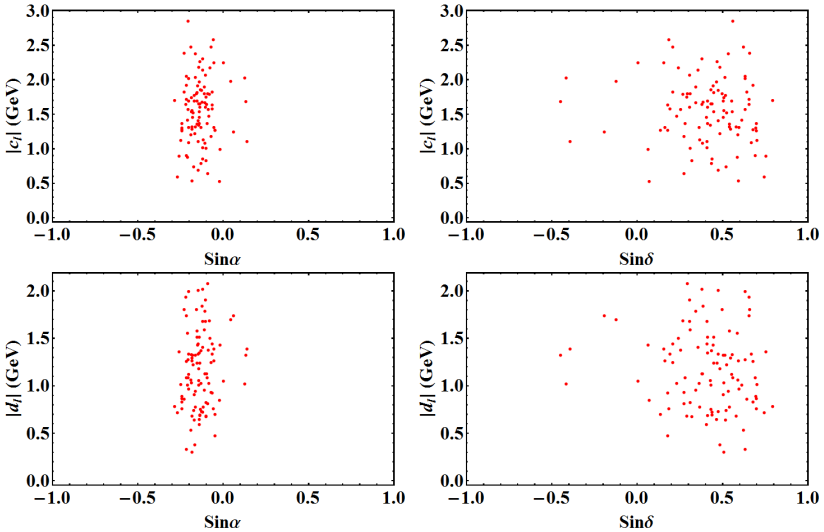

Figure 3.10: Correction parameters as a function of Majorana and Dirac phases while giving correction to the charged lepton mass matrix.

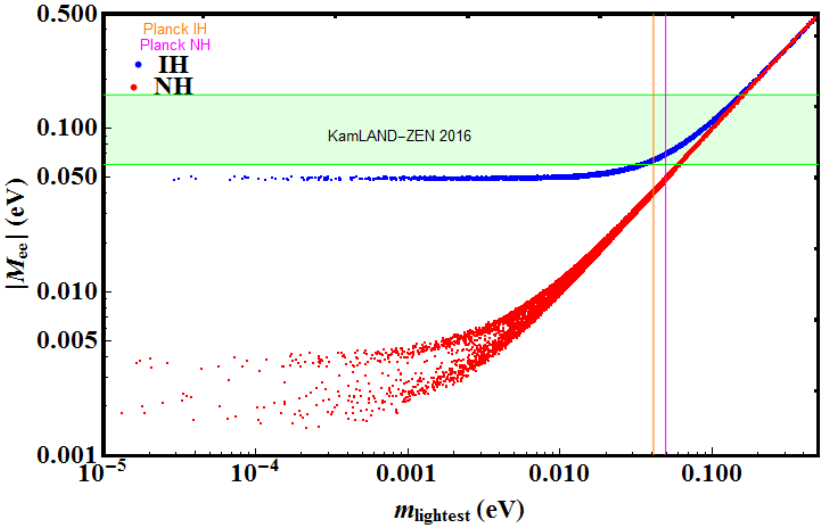

Figure 3.11: Variation of effective neutrino mass with the lightest neutrino mass in the model with neutrino mass correction. The purple line indicates the PLANCK bound on the sum of absolute neutrino masses. The green band shows the KamLAND-ZEN upper bound [63] on the effective neutrino mass.

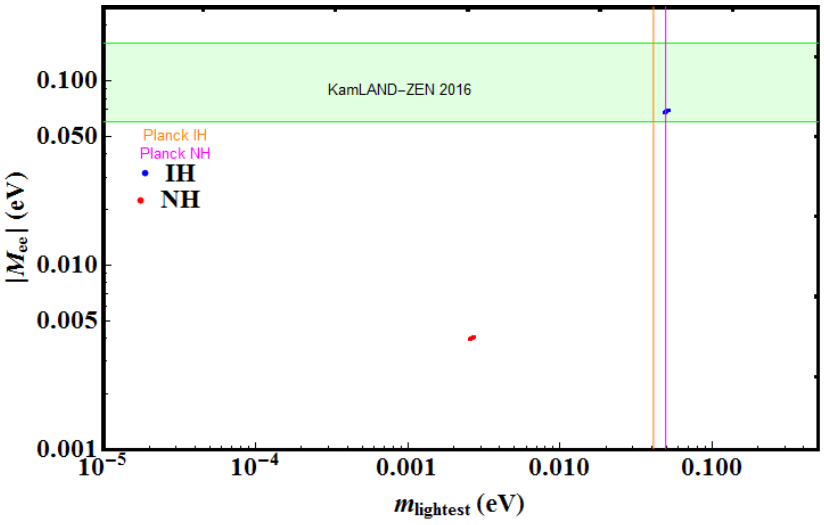

Figure 3.12: Variation of effective neutrino mass with the lightest neutrino mass in the model with charged lepton correction. The purple line indicates the PLANCK bound on the sum of absolute neutrino masses. The green band shows the KamLAND-ZEN upper bound [63] on the effective neutrino mass.

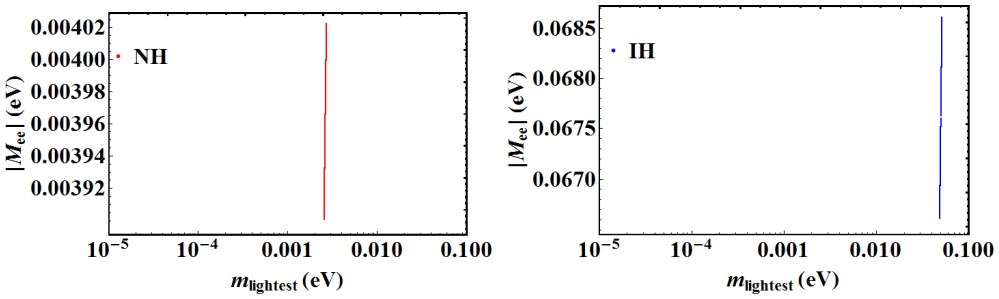

Figure 3.13: Variation of effective neutrino mass with the lightest neutrino mass in the model with charged lepton correction.

ters, numerically evaluated for both the models, we also calculate the respective predictions for neutrinoless double beta decay and plot it as a function of the lightest neutrino mass. Figure 3.11 shows the predictions for effective neutrino mass for both the hierarchies in the model where $\theta_{13} \neq 0$ is generated from neutrino sector itself. As expected, the inverted hierarchy predictions lie very close to the upper bound on M_{ee} from KamLAND-Zen experiment [63]. Similarly, fig 3.12 shows the predictions for effective neutrino mass M_{ee} for the second model where the charged lepton mass matrix is given a correction to generate non-zero θ_{13}. Due to very few number of allowed points in this case, the predicted values of M_{ee} are seen as a dot for both the hierarchies. This is also due to the fact the neutrino mass sum rule Eq. (3.2.12) is valid in this case which restricts the lightest neutrino mass to a small range of values. As can be seen from figure 3.12, the latest KamLAND-Zen data already disfavour this case for inverted hierarchy. If we zoom the points near the two dots in figure 3.12, they look like the points shown in figure 3.13. It is interesting to note that in both the models, the Planck bound on the sum of absolute neutrino mass $\sum_i |m_i| < 0.17$ eV [34] results in an upper bound on the lightest neutrino mass as $m_{\text{lightest}} \leq 0.04939$ eV for normal hierarchy, $m_{\text{lightest}} \leq 0.0414$ eV for inverted hierarchy, if we use the best fit values of mass squared differences. Interestingly this bound almost coincides with the bound from the KamLAND-Zen experiment as seen from figure 3.11. Finally we show the allowed range of dark matter mass and its couplings to leptons from the requirement of satisfying correct dark matter relic abundance criteria in figure 3.14. As expected, higher the values of mediator mass, the larger Yukawa cou-

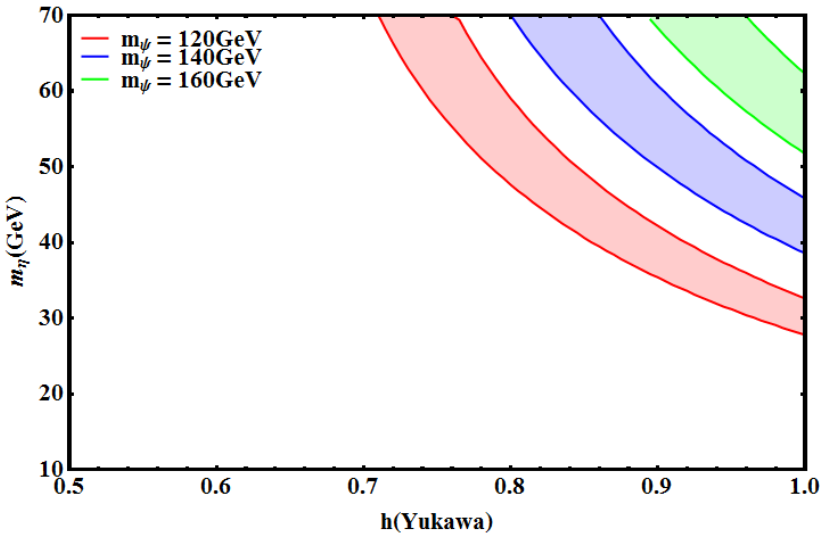

Figure 3.14: Dark matter mass as a function of Yukawa coupling keeping the mediator mass fixed for each plots, such that the constraints on the DM relic abundance is satisfied.

plings are needed to give rise to the correct relic abundance. Such large Yukawa couplings and smaller mediator masses favourable from lepton portal limit of DM will make the charged lepton correction case more favourable. This is because, one needs suppressed Yukawa couplings or large mediator mass in order to generate sub-eV corrections to light neutrino mass, than generating sub-GeV corrections to the charged lepton mass matrix.

3.7 Conclusion

We have studied a TeV scale inverse seesaw model based on S_4 flavour symmetry which can naturally generate correct light neutrino masses with Tri-Bimaximal type mixing at leading order. The model also predicts a neutrino mass sum rule that can further predict the value of the lightest neutrino mass, that can be tested at experiments like neutrinoless double beta decay. Since TBM mixing has already been ruled out by the latest neutrino oscillation data, we consider two possible ways of generating non-zero θ_{13} which automatically take dark matter into account. The idea is based on the scotogenic mechanism of neutrino mass generation, where neutrino mass arises at one loop level with DM particles going

inside the loop. We first give such a one loop correction to the leading order light neutrino mass matrix and numerically evaluate the model parameters from the requirement of satisfying the correct neutrino data. This however, disturbs the mass sum rule prediction of the original model. The dark matter candidate in such a case could either be a singlet neutral fermion or the neutral component of a scalar doublet, depending whichever is lighter. We also study the possibility of generating $\theta_{13} \neq 0$ by giving a correction to the charged lepton sector. Such a case is found to be more constrained from the requirement of satisfying the correct neutrino data. We find much narrower ranges of points in terms of light neutrino parameters which can bring the model predictions closer to the observed data. Consistency with light neutrino data also requires the right diagonalising matrix of charged lepton to have very small mixing angles. The DM candidate in this case is the neutral component of a scalar doublet.

We also study the predictions for neutrinoless double beta decay and found that the charged lepton correction case with inverted hierarchy is disfavoured by the latest KamLAND-Zen data. The predictions for effective neutrino mass in this model is very specific and confined to a tiny region around a particular value of lightest neutrino mass. This is due to the neutrino mass sum rule which forces the lightest neutrino mass to remain within a very narrow range. We also find the allowed parameter space for scalar dark matter from the requirement of producing the correct neutrino data, ignoring the Higgs portal and gauge mediated annihilations. Such lepton portal annihilations are efficient for large Yukawa couplings or smaller mediator masses. Since the same Yukawa couplings and mediator mass go into the one loop correction for both neutrino and charged lepton mass matrix, the charged lepton correction is more favourable from lepton portal scalar DM point of view. As mentioned before, this is due to the fact that large Yukawa or small mediator mass will be able to generate sub-GeV corrections to charged lepton mass matrix more naturally than generating sub-eV corrections to light neutrino mass matrix. Also, the charged lepton correction case is much more predictive, as obvious from a much narrower region of allowed parameter space compared to the model with neutrino mass correction.

Bibliography

[1] Fukuda, S., et al. Constraints on neutrino oscillations using 1258 days of Super-Kamiokande solar neutrino data. *Physical Review Letters*, 86(25):5656, 2001.

[2] Ahmad, Q. R. , et al. Direct evidence for neutrino flavor transformation from neutral current interactions in the Sudbury Neutrino Observatory. *Physical Review Letters*, 89(1):011301, 2002.

[3] Bahcall, J. N., and Pena-Garay, C., Solar models and solar neutrino oscillations, *New Journal of Physics*, 6:63, 2004.

[4] Abe, S., et al. Precision Measurement of Neutrino Oscillation Parameters with KamLAND. *Physical Review Letters*, 100(22):221803, 2008.

[5] Abe, K., et al. Indication of Electron Neutrino Appearance from an Accelerator-produced Off-axis Muon Neutrino Beam, *Physical Review Letters*, 107(4):041801, 2011.

[6] Abe, Y., et al. Indication of Reactor $\bar{\nu}_e$ Disappearance in the Double Chooz Experiment. *Physical Review Letters*, 108(13):131801, 2012.

[7] An, F. P., et al. Observation of electron-antineutrino disappearance at Daya Bay. *Physical Review Letters*, 108(17):171803, 2012.

[8] Ahn, J. K., et al. Observation of Reactor Electron Antineutrinos Disappearance in the RENO Experiment. *Physical Review Letters*, 108(19):191802, 2012.

[9] Adamson, P., et al. Electron neutrino and antineutrino appearance in the full MINOS data sample. *Physical Review Letters*, 110(17):171801, 2013.

[10] Weinberg, S. Baryon- and Lepton-Nonconserving Processes, *Physical Review Letters*, 43(21):1566, 1979.

[11] Minkowski, P. $\mu \to e\gamma$ at a rate of one out of 10^9 muon decays?. *Physics Letters B*, 67(4):421-428, 1977.

[12] Mohapatra, R. N. and Senjanovic, G. Neutrino Mass and Spontaneous Parity Nonconservation. *Physical Review Letters*, 44(14):912, 1980.

[13] Schechter, J. and Valle, J. W. F. Neutrino masses in $SU(2) \cdot U(1)$ theories. *Physical Review D*, 22(9):2227, 1980.

[14] Xing, Z. -z. and Zhao, Z. -z. A review of $\mu - \tau$ flavor symmetry in neutrino physics. *Reports on Progress in Physics*, 79(7):076201, 2016.

[15] Harrison, P. F. and Scott, W. G. Tri-Bimaximal Mixing and the Neutrino Oscillation Data. *Physics Letters B*, 530(1-4):167-173, 2002.

[16] Harrison, P. F. and Scott, W. G. Symmetries and Generalisations of Tri-Bimaximal Neutrino Mixing. *Physics Letters B*, 535(1-4):163-169, 2002.

[17] Harrison, P. F. and Scott, W. G. $\mu - \tau$ reflection symmetry in lepton mixing and neutrino oscillations. *Physics Letters B*, 547(3-4):219-228, 2002.

[18] Shimizu, Y., Tanimoto, M., Watanabe, A. Breaking Tri-bimaximal Mixing and Large θ_{13}. *Progress of Theoretical Physics Supplement*, 126:81, 2011.

[19] Ishimori, H., et al. Non-Abelian Discrete Symmetries in Particle Physics. *Progress of Theoretical Physics Supplement*, 183:1, 2010.

[20] Grimus, W. and Ludl, P. O. Finite flavour groups of fermions. *Journal of Physics A: Mathematical and Theoretical*, 45:233001, 2012.

[21] King, S. F. and Luhn, C. Trimaximal neutrino mixing from vacuum alignment in A_4 and S_4 models. *Journal of High Energy Physics*, 09:042, 2011.

[22] Adhikary, B., Brahmachari, B., Ghosal, A., Ma, E., and Parida, M. K. A_4 symmetry and prediction of U_{e3} in a modified Altarelli-Feruglio model. *Physics Letters B*, 638:345-349, 2006.

[23] Ma, E. and Wegman, D. Nonzero θ_{13} for Neutrino Mixing in the Context of A_4 Symmetry. *Physical Review Letters*, 107:061803, 2011.

[24] Altarelli, G. , Feruglio, F.,Merlo,L., and Stamou, E. Discrete Flavour Groups, θ_{13} and Lepton Flavour Violation. *Journal of High Energy Physics*, 08:021, 2012.

[25] Karmakar, B. and Sil, A. Nonzero θ_{13} and Leptogenesis in a Type-I See-saw Model with A_4 Symmetry. *Physical Review D*, 91:013004, 2015.

[26] Chen, M-C., Huang, J., O'Bryan, J, Wijangco, A. M., and Yu, F. Compatibility of θ_{13} and the Type I Seesaw Model with A_4 Symmetry. *Journal of High Energy Physics*, 02:021, 2012.

[27] Borah, D. Deviations from Tri-Bimaximal Neutrino Mixing Using Type II Seesaw. *Nuclear Physics B*, 876(2):575, 2013.

[28] Borah, D. Type II seesaw origin of nonzero θ_{13}, δ_{CP} and leptogenesis. *International Journal of Modern Physics A*, 29:1450108, 2014.

[29] Borah. M., Borah, D., and Das, M. K., and Patra, S. Perturbations to $\mu-\tau$ Symmetry, Leptogenesis and Lepton Flavour Violation with Type II Seesaw. *Physical Review D*, 90(9):095020, 2014.

[30] Taoso, M., Bertone, G., and Masiero, A. Dark Matter Candidates: A Ten-Point Test. *Journal of Cosmology and Astroparticle Physics*, 03:022, 2008.

[31] Zwicky, F. Spectral displacement of extra galactic nebulae. *Helvetica Physica Acta* , 6:110, 1933

[32] Rubin, V. C. and Ford, W. K. Jr. Rotation of the Andromeda Nebula from a Spectroscopic Survey of Emission Regions. *Astrophysical Journal*, 159:379-403, 1970.

[33] Clowe, D. A direct empirical proof of the existence of dark matter. *Astrophysical Journal*, 648: L109, 2006.

[34] Ade, P. A. R., et al. Planck 2015 results. XIII. Cosmological parameters. *Astronomy and Astrophysics* , 594:A13, 2016.

[35] Ma, E. Verifiable Radiative Seesaw Mechanism of Neutrino Mass and Dark Matter. *Physical Review D*, 73(7):077301, 2006.

[36] Hirsch, M., Morisi, S., Peinado, E., and Valle, J. W. F. Discrete dark matter. *Physical Review D*, 82(11):116003(1)–116003(5), 2010.

[37] Meloni, D., Morisi, S., and Peinado, E. Neutrino phenomenology and stable dark matter with A_4. *Physics Letters B*, 697(4):339-342, 2011.

[38] Ma, E. Dark scalar doublets and neutrino tribimaximal mixing from A_4 symmetry. *Physics Letters B*, 671(3):366-368, 2008.

[39] Boucenna, M. S., Morisi, S., Peinado, E., Valle, J. W. F., and Shimizu, Y. Predictive discrete dark matter model and neutrino oscillations. *Physical Review D*, 86(7):073008, 2012.

[40] Boucenna, M. S., Hirsch, M., Morisi, S., Peinado, E., Taoso, M., and Valle, J. W. F. Phenomenology of Dark Matter from A_4 Flavor Symmetry. *Journal of High Energy Physics*, 05:037, 2011.

[41] Mukherjee, A. and Das, M. K. Neutrino phenomenology and scalar Dark Matter with A_4 flavor symmetry in Inverse and type II seesaw. *Nuclear Physics B*, 913:643-663, 2016.

[42] Borah, D. and Adhikari, R. Abelian Gauge Extension of Standard Model: Dark Matter and Radiative Neutrino Mass. *Physical Review D*, 85(9):095002, 2012.

[43] Bhattacharya, S., Karmakar, B., Sahu, N., and Sil, A. Unifying the flavor origin of dark matter with leptonic nonzero θ_13. *Physical Review D*, 93(11):115041, 2016.

[44] Mohapatra, R. N. and Valle, J. W. F. Neutrino mass and baryon-number nonconservation in superstring models. *Physical Review D*, 34(5):1642, 1986.

[45] Gonzalez-Garcia, M. and Valle, J. W. F. Fast decaying neutrinos and observable flavour violation in a new class of majoron models. *Physics Letters B*, 216(3-4):360-366, 1989.

[46] Mohapatra, R. N. Mechanism for understanding small neutrino mass in superstring theories. *Physical Review Letters*, 56(6):561, 1986.

[47] Antusch, S., Cazzato, E., and Fischer, O. Sterile neutrino searches at future e^-e^+, pp, and ep colliders. *International Journal of Modern Physics A*, 32(14):1750078, 2017.

[48] Dorame, L., Morisi, S.,Pienado, E., Valle, J. W. F., and Rojas, A. D. New neutrino mass sum rule from the inverse seesaw mechanism. *Physical Review D*, 86(5):056001, 2012.

[49] Rodejohann, W. Neutrino-less double beta decay and particle physics . *International Journal of Modern Physics E*, 20(09):1833, 2011.

[50] Altarelli, G. and Feruglio, F. Discrete flavor symmetries and models of neutrino mixing. *Reviews of Modern Physics*, 82:2701, 2010.

[51] King, S. F. and Luhn, C. Neutrino Mass and Mixing with Discrete Symmetry. *Reports on Progress in physics*, 76:056201, 2013.

[52] Hirsch, M., Morisi, S. and Valle, J. W. F. A_4 based tri-bimaximal mixing within inverse and linear seesaw schemes. *Physics Letters B*, 679(5):454-459, 2009.

[53] Kolb, E. W. and Turner, M. S. *The Early Universe*. Elsevier Inc., San Diego, CA. pages 1-547, 1990.

[54] Scherrer, R. J. and Turner, M. S. On the relic, cosmic abundance of stable, weakly interacting massive particles. *Physical Review D*, 33(6):1585, 1986.

[55] Jungman, G., Kamionkowski, M., and Griest, K. Supersymmetric Dark Matter. *Physics Reports*, 267(5-6):195-373, 1996.

[56] Barbieri, R., Hall, L. J., and Rychkov, V. S. Improved naturalness with a heavy Higgs: An Alternative road to LHC physics. *Physical Review D*, 74(1):015007, 2006.

[57] Cirelli, M., Fornengo, N., and Strumia, A. Minimal Dark Matter. *Nuclear Physics B*, 753(1-2):178-194, 2006.

[58] Honorez, L. L. and Yaguna, C. E. A new viable region of the inert doublet model. *Journal of Cosmology and Astroparticle Physics*, 01:002, 2011.

[59] Borah, D. and Cline, J. M. Inert doublet dark matter with strong electroweak phase transition. *Physical Review D*, 86(5):055001, 2012.

[60] Dasgupta, A. and Borah, D. Scalar Dark Matter with Type II Seesaw. *Nuclear Physics B*, 889:637-649, 2014.

[61] Bai, Y. and Berger, J. Lepton Portal Dark Matter. *Journal of High Energy Physics*, 08:153, 2014.

[62] Akerib, D. S., et al. Results from a Search for Dark Matter in the Complete LUX Exposure. *Physical Review Letters*, 118(2): 021303, 2017.

[63] Gando, A., et al. Search for Majorana Neutrinos Near the Inverted Mass Hierarchy Region with KamLAND-Zen. *Physical Review Letters*, 117(8): 082503, 2016.

[64] Esteban, I., Gonzalez-Garcia, M. C., Maltoni, M., Martinez-Soler, I., and Schwetz, T. Updated fit to three neutrino mixing: exploring the accelerator-reactor complementarity. *Journal of High Energy Physics*, 01:087, 2017.